

HD1: Design and Fabrication of a 16 Tesla Nb₃Sn Dipole Magnet

A.R. Hafalia, S.E. Bartlett, S. Caspi, L. Chiesa, D.R. Dietderich, P. Ferracin, M. Goli, S.A. Gourlay, C.R. Hannaford, H. Higley, A.F. Lietzke, N. Liggins, S. Mattafirri, A.D. McInturff, M. Nyman, G.L. Sabbi, R.M. Scanlan, and J. Swanson

Abstract— The Lawrence Berkeley National Laboratory (LBNL) Superconducting Magnet Group has completed the design, fabrication and test of HD1, a 16 T block-coil dipole magnet. State of the art Nb₃Sn conductor was wound in double-layer racetrack coils and supported by an iron yoke and a tensioned aluminum shell. In order to prevent conductor movement under magnetic forces up to the design field, a coil prestress of 150 MPa was required. To achieve this level without damaging the brittle conductor, the target stress was generated during cool-down to 4.2 K by exploiting the thermal contraction differentials between yoke and shell. Accurate control of the shell tension during assembly was obtained using pressurized bladders and interference load keys. An integrated 3D CAD model was used to optimize magnetic and mechanical design and analysis.

Index Terms—Nb₃Sn, Superconducting accelerator magnet.

I. INTRODUCTION

HIGH field superconducting magnets are required for upgrades of particle accelerators such as the LHC, as well as for future hadron colliders at the energy frontier. At the present time, Nb₃Sn is the only practical superconductor available for design fields above 10 Tesla. In a series of magnet tests, LBNL has achieved progressively higher fields using Nb₃Sn in a variety of coil configurations [1]. During the 1980s, pioneering work on wind-and-react technology resulted in the fabrication and test of the D-10 block-coil dipole magnet up to 8 Tesla [2]. In the 1990s, the cos² dipole, D-20, reached 13.5 Tesla [3]. In 2001, the dual-bore common coil dipole RD-3b achieved 14.5 Tesla [4].

The latest LBNL R&D prototype, denominated HD-1, is a block-coil dipole that pushes the limits of accelerator magnet technology to unprecedented levels in terms of magnetic field and associated mechanical stresses. The magnet uses state of the art conductor with a critical current density of 3 kA/mm² at 12 T/4.2K. This conductor is capable of generating fields above 16 Tesla in practical accelerator dipole designs. However, limitations may arise due to conductor degradation

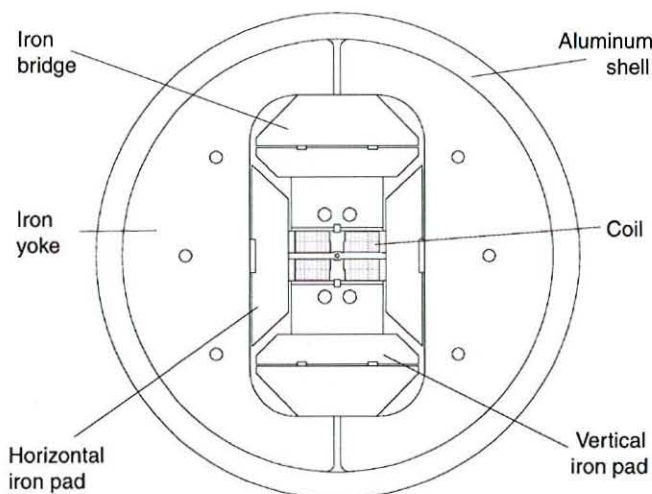


Figure 1: HD1 magnet cross-section. The outer diameter of the shell is 74 cm.

under the mechanical stresses associated with such field levels. HD-1 was designed to investigate these limits using a simple racetrack coil configuration. A support structure based on iron yoke and aluminum shell was selected to withstand the magnetic forces. The shell was pre-tensioned during magnet assembly using bladder and key technology [5], which was developed at LBNL. The water-pressurized, removable bladders provide a precise way of controlling the coil preloads at room temperature. This preload increases at cool-down to a predictable value.

II. MAGNET COMPONENTS

The magnet cross-section, shown in Figure. 1, combines two double-layer racetrack coil modules in a block configuration. Each coil module is wound around an iron pole (island). A 10mm-thick G10 bore plate separates the coils and provides a clear bore of 8 mm in diameter. The support structure is composed of horizontal and vertical iron load pads, iron bridges, iron yokes and aluminum shell. The yoke and loading structure was previously used in the RD series of dual-bore common coil magnets. The components are pre-assembled into two sub-assemblies. The first subassembly, the coil-pack, is composed of the two coil modules, held together

Manuscript received October 20, 2003. This was supported by the Director, Office of Energy Research, Office of High Energy and Nuclear Physics, High Energy Physics Division, U. S. Department of Energy, under Contract No. DE-AC03--76SF00098.

All authors are with the Lawrence Berkeley National Lab, Berkeley, CA 94720 USA (telephone: 510 486 5712, e-mail: rhafalia@lbl.gov.).

by four bolted iron load pads. The second subassembly, the loading structure, is comprised of two iron yoke stacks and an outer aluminum shell. The coil-pack subassembly is inserted in the loading structure, while the spaces between the vertical (Y-) load pads and the yoke stacks are filled by two iron Y-bridges. Clearances are designed between the horizontal (X-) load pads and yokes and between the Y-load pads and the Y-bridges. They provide room for inserting six bladders – two on each X-load pad and one on each Y-Load pad. These bladders, when pressurized, compress the coil-pack both in the vertical and in the horizontal direction. At the same time, the yoke halves are pushed apart and the aluminum shell is pre-tensioned. Six interference load keys (one load key per X-load pad and two load keys per Y-load pad) lock the pre-stress in the entire assembly and allow for bladder removal. During cool-down, the differential thermal contraction between the yoke and the shell produces a significant increase of tension in the shell – resulting in increased compression on the coil-pack. Four aluminum rods, pre-tensioned at room temperature, assure adequate axial pre-stress in order to minimize displacements in the coil end region.

III. CONDUCTOR AND CABLE

The superconducting cable was fabricated at LBNL from 36 strands of Oxford Superconducting Technology (OST) formed by the Restacked Rod Process (RRP) [6]. The critical current density of all the strands was similar - greater than 1.45 kA/mm^2 at $15 \text{ T}/4.2 \text{ K}$, with the self-field correction. The strand and cable parameters are listed in Table I. The standard cabling process at LBNL consists of a double-rolling process, with a low temperature anneal in between the two rolling steps. In the first phase, the cable thickness is slightly above the target cross-section (Cable 864). The cable is then annealed at 200°C for 6 hours and re-rolled to produce the final cable with the desired cross-sectional dimensions (Cable 864R).

TABLE I: STRAND AND CABLE CHARACTERISTICS

Strand Name	Strand Dia. (mm)	Cu to SC Fraction	Sub-elements Dia. (μm)	No. Strands in Cable
6445	0.803	0.68	75-95	4
6555	0.803	0.97	75-95	24
6813	0.803	0.95	75-95	8

Cable No.	MFG.	Cable Compaction (%)	Thickness (mm)	Width (mm)	Cable Pitch Length (mm)
864	Oxford	85.3	1.411	15.75	109
864R	Oxford	88.5	1.361	15.75	109

IV. SUPERCONDUCTING COIL MODULES

Each coil module is a double-layer racetrack with 35 turns in the inner layer (next to the bore plate) and 34 turns in the outer layer (Fig. 2). The turns are tightly wound around an iron island with a single stainless steel spacer added at each end to reduce the local field and assure the highest field remains in

the straight section. The layer-to-layer transition is located along the straight section of the iron pole near the lead end.

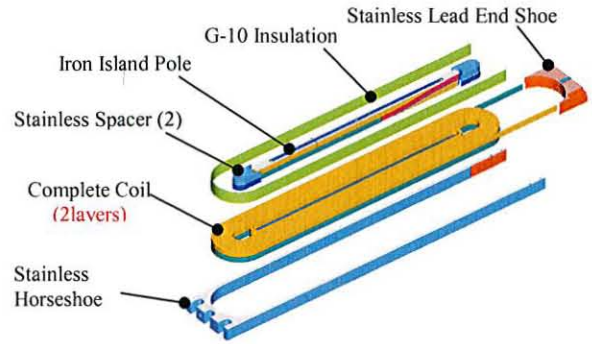


Figure 2: HD-1 coil Module components. Total coil length is 88cm.

A stainless steel horseshoe, initially developed and successfully tested on the smaller coils of our Subscale Magnet Program [7], was used for the first time on a full scale magnet to provide a continuous supporting surface around the coil and an unbroken sealing surface for epoxy impregnation. After winding, the coils were assembled in the reaction fixture and heat treated with the following schedule: 210°C for 100h; 340°C for 48h; and 650°C for 200h. For the heat treatment, the coils were sealed in a stainless steel retort that was continuously purged with Argon gas. After reaction, each coil's instrumentation was connected to the voltage tap/quench heater trace and, then, impregnated with CTD 101 epoxy. The completed coil modules are shown in Figure 3.

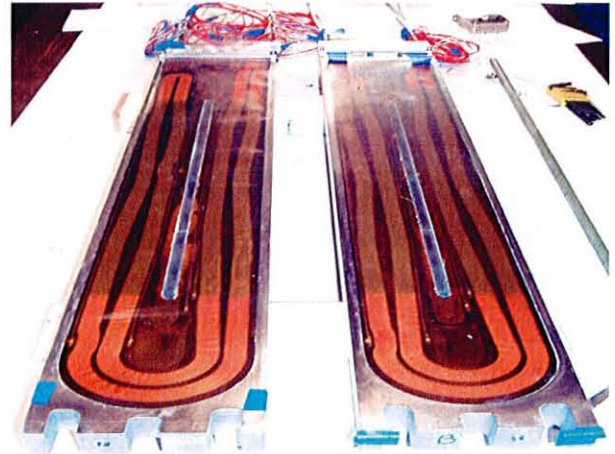


Figure 3: Modules A & B, fully impregnated and with voltage tap/quench heater traces.

V. SUPPORT STRUCTURE

Both coils, sandwiching a 10mm NEMA G-10 boreplate, were stacked between the X- and Y-load pads (Fig. 4, left). A sheet of 3.17mm-thick G-10 "skin" was placed between the outer coil surface of each coil module and Y-load pad. The four load pads were held together with 11.0 mm diameter bolts - torqued to achieve a nominal coil pack size without imparting any significant preload to the coils. The coil-pack pre-assembly was, then, inserted into the shell. (Figure.4, right).



Figure 4: Assembled coil-pack (left) and shell and loading structure (right).

To pre-stress the coil modules in the longitudinal direction, four aluminum rods, with a diameter of 19.0 mm, were inserted through the full-length clearance-holes in vertical pads (Figure. 5, left). Two of the rods were instrumented with strain-gauges to monitor the stress evolution of the coil during assembly, cool-down and operation. Both ends of the rods were secured to 50mm-thick end plates using double-nuts after specially designed rod Z-load rig was used to preload the rods simultaneously during the bladder pressurization process (Fig. 5, right)

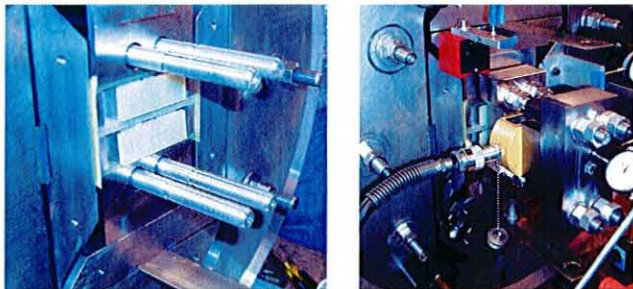


Figure 5: 19.0mm diameter Aluminum rods (left) and Z-load rod hydraulic preloading assembly (right).

VI. MAGNET ASSEMBLY

HD-1 was the first magnet assembled with bladders placed orthogonally. Both vertical (Y-axis) and horizontal (X-axis) preloading was used to produce transverse loading on the coils. A separate, hydraulic preloading assembly was used on the Z-load rods for coil longitudinal pre-loading. Additional components were required to adapt the HD-1 coil-pack to the existing RD-3 loading structure. Horizontal and vertical load pads were fabricated and large iron "Y-bridges" added over the vertical pads in order to fill the gap between the Y-pads and yokes. The vertical bladders and load keys were inserted between the vertical pads and the iron bridges. The horizontal bladders and interference keys were inserted between the horizontal pads and the yokes.

Transverse pre-load was accomplished by pressurizing the bladders with water. For final loading operation, only three of the six bladders (one y-bladder and two of the X-bladders on the same side) were pressurized. For axial pre-stress, the special hydraulically actuated rod-tensioning assembly was bolted to the axial rod ends, at the return end, and pushed against the 50.0mm-thick end plates, which bore directly against the coil module ends. (Figure. 5, right).

The loading schedule required simultaneous pressurization

of the bladders and the axial actuator. The transverse stresses in the shell and the axial stresses in the rods were monitored and recorded from the corresponding strain gages. When the required pre-stress pressures were reached, all the horizontal and vertical load keys were inserted and the nuts at the ends of the rods were tightened. This operation locked in the transverse and axial pre-loads when the pressures in the bladders and actuator were relieved. This permitted the removal of the bladders and actuator assembly. The final assembly of is shown in Fig. 7.



Figure 7: HD-1 final assembly

VII. STRUCTURAL ANALYSIS

A. Design analysis and integration

The Group has developed a fully integrated magnet design and analysis process that has been applied to HD-1. The process begins by uploading three-dimensional baseline coil data into the Pro/Engineer CAD system, where the solid model of the complete coil is automatically generated – turn-by-turn. The magnet components are generated around the coil surfaces creating a complete structural assembly.

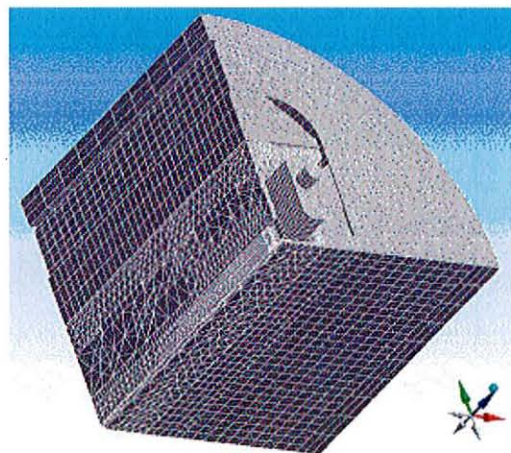


Figure 8: Meshed ANSYS model.

The completed assembly model can be read into, either, the structural analysis program ANSYS (Figure. 8), or the magnetic analysis program, TOSCA. The resultant elemental force vectors from TOSCA's field computations are

superimposed on the ANSYS structural model to obtain the stress and deformation analyses. (Figure. 9).

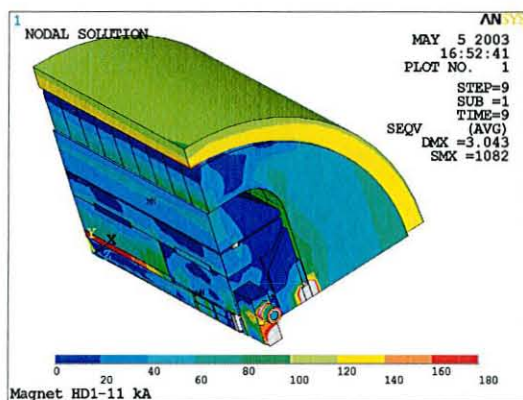


Figure 9: ANSYS Von Mises stress contour plot. Load case: 4.3K + 11kA.

During the design process, numerous ANSYS runs were performed to optimize the design. The aim was to ascertain the adequate pre-stress of the coil to prevent coil separation from the iron island (pole) at full field and to reduce possible axial motion in the ends between coil, island, end-spacers and shoe.

The HD-1 structural analysis simulates the four structural load phases the magnet undergoes during assembly and testing: 1) the 30 Mpa bladder pressurization with preload in the axial rods - stretched 1mm; 2) insertion of load keys; 3) cool-down to 4.3K; 4) Lorentz forces at 11 kA (16 T). The results for each step were compared with the strain gauge measurements taken from the shell and the aluminum rods.

B. Coil Analysis Results

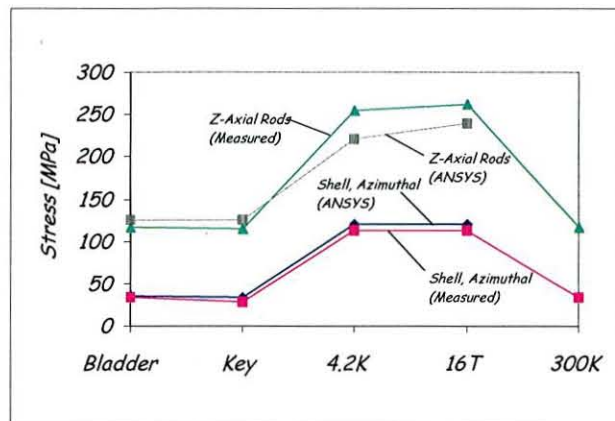
After the loading operation, the coil experiences a compressive stress, σ_x , of 35 MPa in the inner layer and 45 MPa in outer layer (center of each layer). Upon cool-down, σ_x increases to 155 MPa and 160 MPa in the inner and the outer layer, respectively. At full field (11kA) the stress redistributes and varies somewhat linearly from 0 Mpa, next to the pole to 170 MPa near the horseshoe (for both layers).

In the axial (Z) direction, both layers behave similarly. The axial stress, σ_z , retains a maximum value around the magnet-end. During assembly, that stress is compressive (-35 MPa), building up to (-100 MPa after cool-down, and relaxing to -80MPa with Lorentz forces. The axial stress in the straight section is -20MPa during assembly, increasing to -130MPa after cool-down. With Lorentz forces, the axial stress in the straight section develops a gradient varying from +65 MPa of tension near the pole to about 0 MPa next to the shoe. (At the same time, the stress normal to the coil at the pole (σ_x) varies from -40 MPa during assembly to -150 MPa with cool-down to -10 MPa with Lorentz forces.) The increase in axial stress along the pole (in the Z-direction) and the reduction of the normal stress there (in the X-direction) will, most likely, cause training if displacements and slippages are permitted. We have minimized that slippage as much as possible by compressing the coils in the X- and Z-directions.

C. Aluminum Shell Analysis Results

The tension in the aluminum shell will increase from 33 MPa during assembly to 120 MPa at 4.35K and will not change during operation. The results are in very good agreement with the experimental measurements (Figure 10).

Fig. 10. Measured and computed stresses in the shell and in the aluminum



rods, during assembly, cool-down and test.

D. Aluminum Rod Analysis Results

The initial axial stress on the rod is 125 MPa of tension (135 measured). After cool-down the tension in the rod increases to 220 MPa (230 Mpa, measured) and with full Lorentz forces, it is 250 MPa (240 MPa measured).

VIII. CONCLUSIONS

The HD-1 magnet began testing on October 8, 2003. At the time of this paper's submission, the magnet test was still in progress – undergoing the first thermal cycle, but the initial magnet training phase was completed – achieving a peak, measured bore field of 16T (a new world record for a dipole magnet). The structure and magnet are performing very well and seems to be correlating well with the analysis predictions.

REFERENCES

- [1] L. Chiesa et al., "Performance Comparison of Nb₃Sn Magnets at LBNL", IEEE Trans. Appl. Supercond. Vol. 13, no. 2, June 2003, pp. 1254-1257.
- [2] C. Taylor et al., "A Nb₃Sn dipole magnet reacted after winding", IEEE Trans. Magnetics Vol. MAG-21, No. 2, March 1985, pp. 967-970.
- [3] A.D. McInturff et al., "Test results for a High Field (13 T) Nb₃Sn Dipole", Proceedings of the 1997 Particle Accelerator Conference, Vancouver, CA, 1997, p.3212.
- [4] R. Benjegerdes et al., "Fabrication and Test Results of a High Field, Nb₃Sn Superconducting Racetrack Dipole Magnet", Proceedings of the 2001 Particle Accelerator Conference, Chicago, June 2001.
- [5] S. Caspi et al., "The use of Pressurized Bladders for Stress Control of Superconducting Magnets", IEEE Appl. Supercond. Vol. 11, March 2001, pp.
- [6] J. Parrell et al., "High Field Nb₃Sn Conductor Development at Oxford Superconducting Technology", IEEE Trans. Appl. Supercond. Vol. 13, no. 2, June 2000, pp. 3470-3473.
- [7] R.R. Hafalia et al., "A new support structure for high field magnet", IEEE Trans. Appl. Superconduct., vol. 12, no. 1, March 02, pp. 47-50.
- [8] R.R. Hafalia et al., "An Approach for Faster High Field Magnet Technology Development", IEEE Trans. Applied Superconductivity, vol. 13, no. 2, June 2003, pp. 1258-1261.